Downloaded from rsta.royalsocietypublishing.org

PHILOSOPHICAL TRANSACTIONS OF THE ROYAL SOCIETY A MATHEMATICAL, PHYSICAL & ENGINEERING SCIENCES

Line-Narrowing Approaches to Solid State NMR Imaging: Pulsed Gradients and Second Averaging [and Discussion]

J. B. Miller, D. G. Cory, A. N. Garroway, P. Mansfield, D. J. Greenslade, K. J. Packer, R. D. Farrant, J. H. Strange, J. Frahm and E. L. Hahn

Phil. Trans. R. Soc. Lond. A 1990 **333**, 413-426
doi: 10.1098/rsta.1990.0169

Email alerting service

Receive free email alerts when new articles cite this article - sign up in the box at the top right-hand corner of the article or click **here**

To subscribe to *Phil. Trans. R. Soc. Lond. A* go to:
http://rsta.royalsocietypublishing.org/subscriptions

This journal is © 1990 The Royal Society

Downloaded from rsta.royalsocietypublishing.org

Line-narrowing approaches to solid state NMR imaging: pulsed gradients and second averaging

By J. B. Miller, D. G. Cory and A. N. Garroway
Code 6122, Naval Research Laboratory, Washington, D.C., 20375-5000, U.S.A.

There are questions in materials sciences which can be addressed by NMR imaging. However, not all materials exhibit sufficient molecular motion to reduce dipolar couplings to the level at which the familiar techniques of medical NMR imaging are appropriate. For the more general case of these less mobile materials, line-narrowing methods, specialized to imaging, are appropriate. We have earlier demonstrated that such imaging sequences adequately overcome the fundamental dipolar broadening in engineering polymers; however, these sequences are subject to certain practical limitations which we address.

We present a class of homonuclear line-narrowing imaging methods which intercalate short gradient pulses (*ca.* 5 μs) into the RF pulse sequence. Such a strategy improves spatial resolution and signal sensitivity by reducing extraneous broadening from off-resonance effects. In a further implementation, the chemical shift and susceptibility terms in the spin hamiltonian are suppressed by 'second averaging' about a particular axis, while the hamiltonian for the gradient pulses is aligned along that axis: the result is a further improvement in spatial resolution.

Prospects for the future of solid state NMR imaging are considered.

Introduction

NMR imaging is underpinned by a deceptively simple idea: spatially varying magnetic fields encode the positions of nuclear spins into their Larmor precession frequencies (or, perhaps, RF nutation frequencies); the nuclei are excited; and the signal intensities at these spatial frequencies are recorded and rearranged to construct an image. Since 1973 (Lauterbur 1973) medical imaging has progressed from what some thought was a laboratory curiosity to a clinically significant diagnostic tool in routine use at all major medical centres. Soft tissue NMR images of astonishing clarity are obtained and, with specialized approaches, images can be acquired in fractions of a second. And, as this symposium demonstrates, important insights into the metabolism of normal and diseased cells are now available by chemical shift imaging.

The first solid state NMR images also date back to 1973 (Mansfield *et al.* 1973; Mansfield & Grannell 1973). Why then has there not been comparable progress in the imaging of non-biological systems, in particular heavily protonated engineering polymers? Certainly, the priority and commitment for human health care overwhelm the concerns for materials sciences. From a technical standpoint, however, the distinction between medical and materials imaging is that rapid

The Royal Society is collaborating with JSTOR to digitize, preserve, and extend access to *Philosophical Transactions: Physical Sciences and Engineering.* www.jstor.org

Downloaded from rsta.royalsocietypublishing.org

molecular motion fortuitously attenuates many of the line-broadening mechanisms in biological systems which are, predominately, water. In materials, and especially rather rigid materials such as glassy and crystalline organic polymers, these broadening mechanisms prevail: in all but the most mobile materials, one must address these line-broadening issues. Hence medical imaging is able to take advantage of liquid state NMR methods while some, but not all, materials science applications will require solid state NMR approaches. Such distinctions dictate that the materials imaging approach will be different, though not necessarily more difficult, than the comparable approaches in medical magnetic resonance imaging (MRI). Although the requisite RF pulse sequences are more cumbersome in the line-narrowing approaches to be presented, solid state imaging generally avoids the problems of motional artefacts, patient throughput, electromagnetic exposure limits and other practical issues which shape the medical MRI procedures. Moreover, in the solid state, one has available that additional information which is averaged to zero by molecular motions in the liquid state: manipulation of this additional information in the solid state can, in principle, provide additional means of image contrast.

Line broadening in solids

Relevant NMR broadening mechanisms include: (i) magnetic dipolar coupling (homonuclear, heteronuclear); (ii) chemical shift (isotropic, anisotropic); (iii) magnetic susceptibility. Lifetime broadening (e.g. spin lattice relaxation, T_1) certainly contributes, though one has far less control over that interaction. To this list of intrinsic broadening mechanisms may be added the extrinsic broadening from the inhomogeneity of the static magnetic field.

For an organic solid rather rich in protons, a typical dipolar linewidth is perhaps 40 kHz or 1 mT (10 G). In the presence of such a coupling, resolving two protons a distance of 100 μm apart would require a gradient of 10 T m^{-1} (1000 G cm^{-1}). Across a 1 cm specimen in such a magnetic field gradient, the proton Larmor frequency varies by *ca.* 4 MHz. Such a brute force approach requires detecting precessional frequencies across a formidable bandwidth, with a corresponding increase in the receiver noise. And of course one must somehow excite the nuclear spins over a bandwidth of 4 MHz, in this example. None the less, methods using large gradients have been demonstrated (Samoilenko *et al.* 1978, 1988; J. H. Strange, this symposium).

In general, any imaging modality requires contrast, spatial resolution, and an adequate signal-to-noise ratio (SNR). Since many materials, including biological systems, have essentially a uniform spin density (though the chemistry may vary greatly across the sample), one must build a contrast mechanism into the NMR imaging procedure. This can be achieved by preceding the imaging sequence with an excitation scheme which emphasizes spins with, say, a particular NMR relaxation time or chemical shift. Another strategy is to build this contrast selectivity directly into the imaging sequence, e.g. so that the image is T_1- or T_2-weighted as in MRI. To increase spatial resolution and to improve the SNR, one prolongs the timescale over which the spins are allowed to precess in the imaging gradients and to be observed: it is therefore desirable to remove all extraneous line-broadening mechanisms.

A number of approaches have been taken to the dipolar broadening. The most convenient, though not universal strategy, is to restrict attention to systems with substantial molecular motions (Chang & Komoroski 1989; Nieminen & Koenig 1990;

PHILOSOPHICAL TRANSACTIONS OF THE ROYAL SOCIETY A MATHEMATICAL, PHYSICAL & ENGINEERING SCIENCES

PHILOSOPHICAL TRANSACTIONS OF THE ROYAL SOCIETY A MATHEMATICAL, PHYSICAL & ENGINEERING SCIENCES

Downloaded from rsta.royalsocietypublishing.org

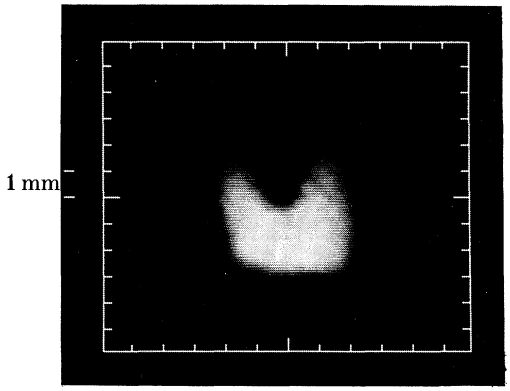

Figure 1. Two-dimensional ^{1}H image of a polyacrylic specimen of dimensions $4.5 \times 5.5 \times 16$ mm. A notch has been cut out parallel to the long direction. The image was obtained by back projection from 18 projections and no slice selection was employed. The refocused gradient methods for homonuclear (Miller & Garroway 1989*a*) spin systems remove chemical shift-like interactions, as well as the respective dipolar couplings. For the homonuclear decoupling sequence used here, the residual line width depends on the resonance offset and therefore the spatial resolution deteriorates across the image: the present paper is concerned with remedies to this effect.

Hall & Rajanayagam 1987) or arrange a penetrant which is itself motionally narrowed (Rothwell *et al.* 1984; Ackerman *et al.* 1988). The apparent gradient may be artificially increased by following the evolution of a multiple-quantum coherence (Garroway *et al.* 1984). Magic angle sample spinning is sufficient (Cory *et al.* 1988; Cory *et al.* 1989; Veeman & Cory 1989) to remove some dipolar couplings, and has the added advantage that the isotropic chemical shift is preserved and can thereby provide a contrast mechanism, while the anisotropic part is averaged to zero. The approach discussed here is to use coherent RF line-narrowing methods to remove some or most of these interactions. We specialize to homonuclear line-narrowing (Haeberlen 1976; Mehring 1983); heteronuclear methods have been demonstrated (Szeverenyi & Maciel 1984; Miller & Garroway 1989*b*; Cory & Veeman 1989), as well as homonuclear line-narrowing combined with magic angle sample spinning (Veeman & Cory 1989; Cory *et al.* 1988). There are also methods which accept the line broadening, but trade-off signal sensitivity for spatial resolution (Emid & Creyghton 1985; Rommel *et al.* 1990).

Imaging by homonuclear line narrowing has already been demonstrated (Veeman & Cory 1989; Cory *et al.* 1988; Wind & Yannoni 1979; Mansfield *et al.* 1973; Mansfield & Grannell 1973, 1975; De Luca 1984; De Luca & Maraviglia 1986; De Luca *et al.* 1986; Chingas *et al.* 1986; McDonald *et al.* 1987). Imaging methods (McDonald & Tokarczuk 1989; Bendel 1985; Cho *et al.* 1985; Miller & Garroway 1986, 1989*a*) have been presented earlier in which the broadening linear in the spin operator I_z (chemical shift, susceptibility, static field inhomogeneity) can be removed by 'refocused gradient imaging' and analogous methods for both homonuclear and heteronuclear cases; there an effective field is periodically reversed to remove chemical shift-like terms over some characteristic period, while an oscillatory or bipolar gradient is synchronized with the reversal of the effective field so that the phase gain from the imaging gradient increases monotonically to preserve spatial information. Figure 1 presents a proton NMR image of a $4.5 \times 5.5 \times 16$ mm polyacrylic specimen for which refocused gradient imaging methods were used. Experimental details appear in

Downloaded from rsta.royalsocietypublishing.org

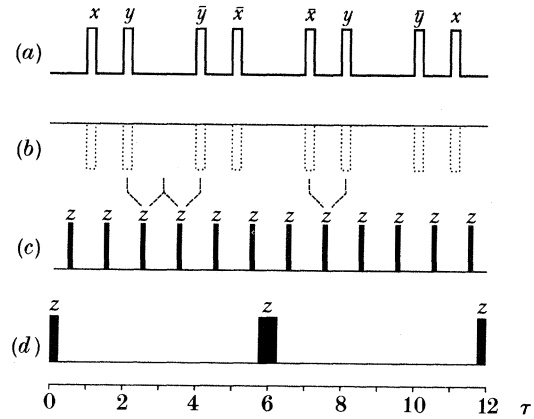

Figure 2. (*a*) The MREV-8 RF pulse sequence; x, y, $\bar{x}$, and $\bar{y}$ represent $\frac{1}{2}\pi$ pulses in phase quadrature with one another. In (*b*) is a continuously applied resonance offset; the dotted lines during the RF pulse indicate that under experimental conditions ($\frac{1}{2}\pi$ pulse length of 2.5 μs and 12τ cycle time of 60 μs), the effect of the resonance offset on the RF pulses is not significant. In (*c*) the continuous resonance offset is represented (Miller *et al.* 1989) as a series of pulsed rotations about z. In this zeroth-order average hamiltonian approximation, the z pulses emulate an RF phase shift, spoiling the quadrature relation among the RF pulses; see ahead to figure 4. In (*d*) are shown pulsed gradients installed in the I_z windows of the 6τ subcycles of the MREV-8 sequence.

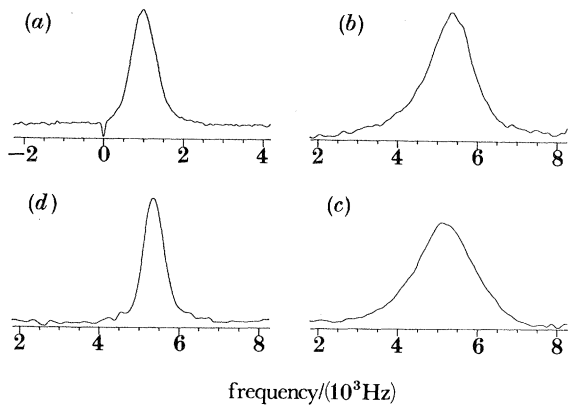

Figure 3. These ^{1}H spectra (Miller *et al.* 1989) of Mylar film demonstrate the origin of the off-resonance line-broadening under MREV-8 decoupling sequence. In (*a*) resonance offset is set to 2 kHz; in (*b*) 11.8 kHz and the resulting linewidth has increased substantially over that in (*a*). (The axes are labelled in unscaled hertz; here the MREV-8 scale factor is about 2.) In (*c*) the resonance offset is 2 kHz but an RF phase shift of $15.4°/\tau$ (cf. figure 2*c*) has been introduced; resolution is comparable with the continuous resonance offset case (*b*). In (*d*) phase shifts of 49° have been inserted in the I_z windows, cf. figure 2*d*, to give a comparable resonance offset to the continuous case (*b*), but with a resulting line shape comparable with, and somewhat better than, the near-resonance condition of (*a*).

Miller & Garroway (1989*a*). All data presented here were obtained on a home built spectrometer operating at 100 MHz for protons. In figure 1 resolution is about 450 μm.

PHILOSOPHICAL TRANSACTIONS OF THE ROYAL SOCIETY A MATHEMATICAL, PHYSICAL & ENGINEERING SCIENCES
PHILOSOPHICAL TRANSACTIONS OF THE ROYAL SOCIETY A MATHEMATICAL, PHYSICAL & ENGINEERING SCIENCES

Downloaded from rsta.royalsocietypublishing.org

Imaging by improved homonuclear decoupling

For the line-narrowing sequence used in figure 1 and earlier work, we used the MREV-8 sequence (Mansfield 1971; Rhim *et al.* 1973*a*, *b*) and variants based on that sequence. In this paper we address one of the practical limitations of the MREV-8 sequence for imaging and demonstrate one appropriate solution. In general the line-narrowing ability of the MREV-8 sequence deteriorates as one moves off resonance. Earlier detailed studies (Garroway *et al.* 1975) on single crystal CaF_2 showed the residual ^{19}F MREV-8 line width actually improved from 140 to 40 Hz on moving from resonance to 0.5 kHz off resonance: for offsets from 0.5 kHz to 5 kHz, the line width then deteriorated monotonically from 40 to about 200 Hz. Although this deterioration off resonance is not a fatal problem for imaging, it is certainly a complication, since the residual line width determines the spatial resolution and hence the spatial resolution will vary across the specimen. (In this above example, the improvement in line-narrowing ability for offsets out to 0.5 kHz arises from 'second averaging' (see below).)

Where does this off-resonance broadening term arise? Note that the resonance offsets (e.g. a maximum of 5 kHz in above example) are not that different from the reciprocal of the MREV-8 cycle time, 13 kHz; that is, over the MREV-8 cycle, there is a very significant gain in phase just due to resonance offset and so the resonance offset is *not* insignificant in comparison to the dipolar interaction we wish to remove. This is just the régime in which we wish to operate for imaging purposes, to make fullest use of the entire Nyquist bandwidth.

To qualitatively examine the effects of a resonance offset, it is instructive (Miller *et al.* 1989) to visualize the effect of a continuous resonance offset during the MREV-8 windows as a set of discrete pulsed rotations about the z axis. Figure 2*a* shows a standard MREV-8 sequence. Though a resonance offset will tip the effective field of the RF pulses out of the xy plane, we have determined (Miller *et al.* 1989) that this effect is *not* responsible for the deterioration in line narrowing with increasing resonance offset; figure 2*b* indicates the offset is effectively zero (dotted line) during the RF pulses. In figure 2*c*, the resonance offset is represented as a series of pulsed rotations about the z axis; that is, in each τ interval a z pulse is applied, giving the same precession as would the continuous gradient over the period τ. Since the rotations about the z axis are equivalent to a phase advance between RF pulses, the x, y, $\bar{x}$ and $\bar{y}$ pulses are, in this sense, no longer in quadrature. We have experimentally verified (Miller *et al.* 1989) that this apparent phase advance does indeed account for the deterioration of line narrowing under our experimental conditions. Figure 3*a* presents the MREV-8 proton spectrum of a Mylar film [poly(ethylene terephthalate)] 2 kHz off resonance, while the linewidth increases by a factor of two on moving out to 11.8 kHz off resonance (figure 3*b*). Spectra are shown in unscaled Hertz and the MREV-8 scale factor is about 2. In figure 3*c* the resonance offset is 2 kHz, and a digital phase shifter has advanced phases of the RF pulses by 15.4 °/τ, equivalent to a 11.8 kHz resonance offset. Note that the MREV-8 line width by the phase advance method (figure 3*c*) is essentially equivalent to the line width for the (continuous) resonance offset case (figure 3*b*) thus qualitatively verifying this simple physical picture of the deterioration of line narrowing.

Some windows in the MREV-8 sequence are more sensitive than others to changes in the RF phase. Phase shifts in the small windows affect formation of the solid echoes. To zeroth order, a phase advance between the two 6τ subcycles

Downloaded from rsta.royalsocietypublishing.org

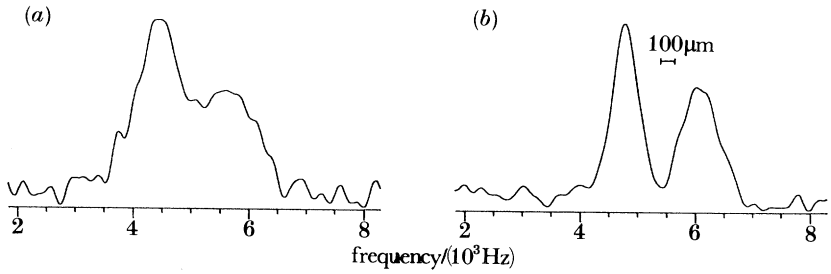

Figure 4. One-dimensional ^{1}H images (Miller *et al.* 1989) of two 130 μm thick Mylar films separated by 560 μm. (*a*) Under the MREV-8 sequence and a continuous gradient the two films are not resolved; in (*b*) with the pulsed field gradient sequence of figure 2*d*, the two films are quite well resolved. The time-averaged gradient in (*b*) is 3 kHz mm^{-1} for protons, and, to avoid artefacts near zero frequency, the sample was displaced from the centre of the gradient coils.

comprising the MREV-8 sequence does not compromise the overall line-narrowing capability; the pulse timing is indicated in figure 2*d*. In figure 3*d* an RF phase advance of 49° has been installed in each of the two I_z windows, cf. figure 2*d*. Note that although the apparent offset is again about 11.8 kHz, the line width is comparable with, and slightly less than, the near-resonance value (figure 3*a*).

Therefore we can arrange to use pulsed magnetic field gradients in lieu of a 'steady' gradient and, further, to insert these gradient pulses in the long (I_z) windows. Figure 4 (Miller *et al.* 1989) presents a one-dimensional ^{1}H image of two sheets of 130 μm thick Mylar film, separated by a 560 μm thick inert spacer. Under MREV-8 line narrowing, the two sheets are unresolved with a steady gradient (figure 4*a*), but are quite well resolved (figure 4*b*) when 3.5 μs pulsed field gradients are used as above.

The use of short (*ca.* 3–5 μs) pulsed field gradients in the MREV-8 line narrowing sequence increases the effective image bandwidth. To increase spatial resolution still further, it is desirable to suppress other broadening mechanisms, such as chemical shift, susceptibility and static field inhomogeneity terms; these terms, linear in the I_z spin operator, are normally preserved by the MREV-8 sequence. One straightforward approach to removing these linear terms is to combine refocused gradient imaging (Cory & Veeman 1989; Miller & Garroway 1989*a*) with pulsed gradients. Under such conditions the polarity of the gradient pulses is alternated as the sign of the chemical shift effective field is reversed by the RF pulse sequence. Use of pulsed gradients in refocused gradient imaging leads to improved spatial resolution and bandwidth as shown by the proton image in figure 5. The phantom was machined from Ultem (polyether imide) and consists of a circular base 9 mm in diameter by 1.9 mm thick, a rectangular layer $6.2 \times 6.5 \times 2.0$ mm thick, and a second layer of smaller rectangles parallel to the rectangle in the first layer. The smaller rectangles are 2.2 mm thick and are separated from each other by 1.6 mm. A 16-pulse sequence (Cho *et al.* 1985) has been used for refocused gradient imaging of solids and is based on a sequence proposed by Mansfield & Grannell (1975). The image is constructed from 60 projections. The features of the phantom are quite clear; in plane resolution is 160 μm, and no slice selection was used.

PHILOSOPHICAL TRANSACTIONS OF THE ROYAL SOCIETY A MATHEMATICAL, PHYSICAL & ENGINEERING SCIENCES
PHILOSOPHICAL TRANSACTIONS OF THE ROYAL SOCIETY A MATHEMATICAL, PHYSICAL & ENGINEERING SCIENCES

Downloaded from rsta.royalsocietypublishing.org

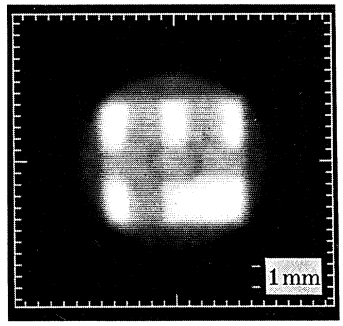

Figure 5. Refocused gradient imaging with pulsed gardients was used to obtain a proton image of an Ultem (polyether imide) phantom, comprising a circular base 9 mm in diameter by 1.9 mm thick, a rectangular layer $6.2 \times 6.5 \times 2.0$ mm thick, and a second layer of smaller rectangles parallel to the rectangle in the first layer. The smaller rectangles are 2.2 mm thick and are separated from each other by 1.6 mm. No slice selection was used and so the small rectangles appear against the background of the larger rectangle and the cylindrical section. A 16-pulse sequence (Cho *et al.* 1985) has been used for refocused gradient imaging of solids and is based on a sequence proposed by Mansfield & Grannell (1975). Resolution is 160 μm.

Figure 6. Proton time domain signals in the two receiver channels are shown for (*a*) the free induction decay (FID), (*b*) MREV-8 sequence and (*c*) second averaged MREV-8 sequence for ferrocene. The horizontal timescale spans 31 ms. The second averaged MREV-8 RF sequence is that of figure 7, with the removal of the gradient pulses.

Second averaging

A further procedure (Cory *et al.* 1990) to removing these linear terms is through 'second averaging'. One conventionally regards (Haeberlen 1976; Mehring 1983) the MREV-8 sequence as a coherent averaging process and views the evolution of the spin system under the effects of an average hamiltonian in a toggling reference frame determined by the MREV-8 sequence. This average hamiltonian can then be equated to an effective field governing the average spin evolution over the course of a pulse cycle. Other perturbing interactions not included in the average hamiltonian provide additional or 'second' averaging and will average to zero the components of the effective field of the average hamiltonian which are perpendicular to and also smaller than the effective field of the perturbing interaction. Hence explicit introduction of a well-chosen perturbation can remove some of the less-desirable terms in the average hamiltonian. The particulars of second averaging are well presented in the literature (Pines & Waugh 1972).

Figure 6 contrasts the time domain signals for polycrystalline ferrocene for a free induction decay (following a single $\frac{1}{2}\pi$ pulse), an MREV-8 sequence and a second averaged MREV-8 sequence. It is clear from the prolonged decay that the second averaging removes further broadening terms (chemical shift, susceptibility, magnet inhomogeneity) from the unmodified MREV-8 sequence.

Downloaded from rsta.royalsocietypublishing.org

Having demonstrated the utility of second averaging the MREV-8 sequence, we explore a strategy for imaging: (i) perturb the MREV-8 sequence by a second averaging field perpendicular to the effective field, $I_z - I_x$, of the chemical shift terms in the MREV-8 sequence to average those latter terms to zero; (ii) apply the imaging gradient parallel to the second averaging field so that imaging is retained; (iii) avoid reintroducing the line broadening terms which were removed by the native MREV-8 sequence and; (iv) retain the capability of large resonance offsets attained by pulsed field gradients.

One of the many possible implementations (Cory *et al.* 1990) is the pulse sequence of figure 6. The second averaging field along $(I_z + I_x)$ is created by altering the phase relation between selected RF pulses by a phase 'toggle' Φ. Cross terms between this phase toggle and the dipolar coupling vanish to zeroth order in the average hamiltonian approximation. By altering the sign of the gradient pulses as shown in figure 7, the effective imaging gradient is placed along $(I_z + I_x)$. Of course, this gradient also provides an effective second averaging field which adds parallel or anti-parallel to the field due to the phase toggle. For some value of resonance offset, the net second averaging field will be zero, and one can, for example, arrange to place this (predictable) dead spot outside the region of interest in the image. Figure 7 also presents a proton image for a 6.35 mm outer diameter poly(methyl methacrylate) cylindrical phantom of wall thickness 0.79 mm, in which a slot has been cut. The MREV-8 cycle time was 60 μs with 2.5 μs $\frac{1}{2}\pi$ RF pulses. The RF phase shifts were implemented by a Merrimac digital phase shifter and the gradient driver was a Techron 7560 audio amplifier. The gradient coil, based on a design by Turner (1988), produces a gradient of 0.3 T m^{-1} (30 G cm^{-1}) at 20 A. The gradient pulse rise time of about 3 μs appears to be limited by the amplifier slew rate. The resolution in this image derives from our suppression of chemical shift, susceptibility and magnet inhomogeneity terms, in addition to the usual homonuclear dipolar broadening.

Future solids imaging

MRI has spawned an apparent variety of instruments, and yet they all essentially accommodate the canonical human body with associated well-known relaxation times. We anticipate much wider diversity of specialized instrumentation and approaches for materials imaging: the machines will likely be purpose-built for the particular task. Some applications, such a process control or quality control and testing, might be characterized by very simple, quite restricted instruments. Full three-dimensional imaging may be quite irrelevant, especially in a quality control environment in which the overall geometry and average morphology are already explicitly defined and one wishes to examine whether some specific features deviate from the norm. Other applications might include characterizing defects in solids: it may be that only the general size distribution or connectivity of defects is important, and not the individual locations of such defects: paradigms include defects in ceramics and the pore structure in oil-bearing rock. We have elsewhere demonstrated an approach (Cory & Garroway 1990) using restricted diffusion which reports size features below that dictated by the conventional MRI signal-to-noise limit.

For these line-narrowing approaches, the RF field strength should be greater than or perhaps comparable to the dipolar coupling, and scaling up from specimens of 1 cm linear dimensions to even 10 cm on a side places rather substantial, but not

PHILOSOPHICAL TRANSACTIONS OF THE ROYAL SOCIETY A MATHEMATICAL, PHYSICAL & ENGINEERING SCIENCES
PHILOSOPHICAL TRANSACTIONS OF THE ROYAL SOCIETY A MATHEMATICAL, PHYSICAL & ENGINEERING SCIENCES

Downloaded from rsta.royalsocietypublishing.org

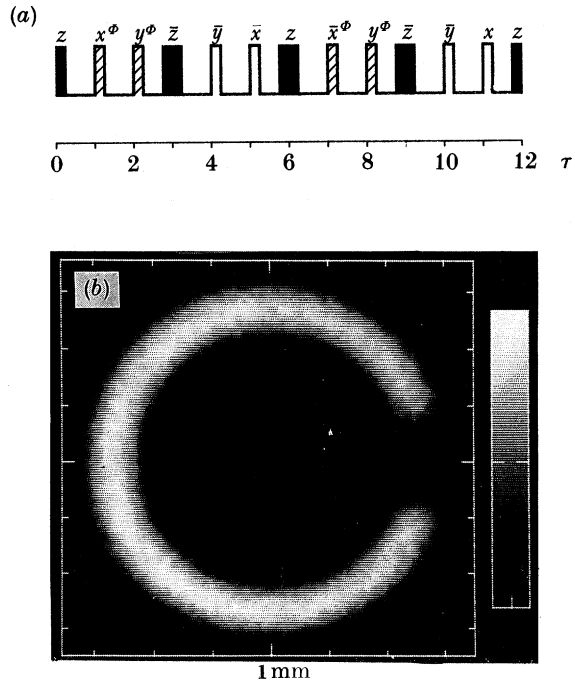

Figure 7. Proton solid state imaging (Cory *et al.* 1990) by second averaging. The MREV-8 RF pulse sequence, top, is modified for second averaging and imaging. To induce second averaging of the chemical shift, susceptibility and magnet inhomogeneity terms which appear as $(I_z - I_x)$ about an orthogonal axis, $(I_z + I_x)$, a phase toggle Φ is applied to pairs of RF pulses as indicated: x^{Φ} denotes a $\frac{1}{2}\pi$ RF pulse which has been advanced by Φ from the x axis. The position and polarity of the gradient pulses, z and $\bar{z}$, are also arranged to produce an effective field about $(I_z + I_x)$ and so the chemical shift-like terms are second averaged by the sum of the gradient and the phase shift terms. Also shown is the ^{1}H image of a 6.35 mm OD poly(methyl methacrylate) cylinder from which a 1.59 mm slot has been machined. No slice selection was used. The image was reconstructed from 64 back projections.

unphysical requirements on RF power: 1 MW narrow-band transmitters are achievable. But, at some point, one might wish to examine specimens too large to fit into an RF coil or even into a magnet: to this end, methods which allow solid state imaging outside an RF coil (Miller & Garroway 1989*c*), by means of the gradient of the RF field and, even, outside the magnet (Samoilenko *et al.* 1987, 1988) are desirable.

This work was sponsored in part by the Office of Naval Research. D.G.C. is a National Research Council/Naval Research Laboratory postdoctoral research associate. Dr R. Turner (National Institutes of Health) kindly provided the coil design for the pulsed gradient coil used here.

References

Ackerman, J. L., Garrido, L., Ellingson, W. A. & Weyand, J. D. 1988 The use of NMR imaging to measure porosity and binder distributions in green-state and partially sintered ceramics. *Proceedings of the Conference on Nondestructive Testing of High Performance Ceramics*, Am. Ceram. Soc., p. 88.

Bendel, P. 1985 Echo projection imaging – a method to obtain NMR images undistorted by magnetic field inhomogeneities. *IEEE Trans. Med. Imaging* **MI-4**, 114.

Downloaded from rsta.royalsocietypublishing.org

Chang, C. & Komoroski, R. A. 1989 NMR imaging of elastomeric materials. *Macromolecules* **22**, 600.

Chingas, G. C., Miller, J. B. & Garroway, A. N. 1986 NMR imaging of solids. *J. magn. Reson.* **66**, 530.

Cho, H. M., Lee, C. J., Shykind, D. N. & Weitekamp, D. P. 1985 Nutation sequences for magnetic resonance imaging in solids. *Phys. Rev. Lett.* **55** 1923.

Cory, D. G., van Os, J. W. M. & Veeman, W. S. 1988 NMR imaging of rotating solids. *J. magn. Reson.* **76**, 543.

Cory, D. G., Reichwein, A. M., van Os, J. W. M. & Veeman, W. S. 1988 NMR imaging of rigid solids. *Chem. Phys. Lett.* **143**, 467.

Cory, D. G. & Veeman, W. S. 1989 ^{13}C NMR imaging of solids with magic angle sample spinning. *J. Phys.* E. **22**, 180.

Cory, D. G., de Boer, J. C. & Veeman, W. S. 1989 Magic angle spinning ^{1}H NMR imaging of polybutadiene/polystyrene blends. *Macromolecules* **22**, 1618.

Cory, D. G. & Garroway, A. N. 1990 Measurement of translational displacement probabilities by NMR: an indicator of compartmentation. *Magn. Reson. Med.* **14**, 435.

Cory, D. G., Miller, J. B. & Garroway, A. N. 1990 Multiple-pulse methods of ^{1}H NMR imaging of solids: second averaging. *Molec. Phys.* **70**, 331.

De Luca, F. 1984 Full-rotating frame NMR imaging. *Lett. Nuovo Cim.* **39**, 390.

De Luca, F., Nuccetelli, C., De Simone, B. C. & Maraviglia, B. 1986 NMR imaging of a solid by the magic-angle rotating-frame method. *J. magn. Reson.* **69**, 496.

De Luca, F. & Maraviglia, B. 1986 Magic-angle NMR imaging in solids. *J. magn. Reson.* **67**, 169.

Emid, S. & Creyghton, J. H. N. 1985 High resolution NMR imaging in solids. *Physica* B **128**, 81.

Garroway, A. N., Mansfield, P. & Stalker, D. C. 1975 Limits to resolution in multiple pulse NMR. *Phys. Rev.* B **11**, 121.

Garroway, A. N., Baum, J., Munowitz, M. G. & Pines, A. 1984 NMR imaging in solids by multiple-quantum resonance. *J. magn. Reson.* **60**, 337.

Haeberlen, U. 1976 Advances in magnetic resonance, Suppl. 1. In *High resolution NMR in solids*. New York: Academic Press.

Hall, L. D. & Rajanayagam, V. 1987 Thin-slice, chemical-shift imaging of oil and water in sandstone rock at 80 MHz. *J. magn. Reson.* **74**, 139.

Lauterbur, P. C. 1973 Image formation by induced local interactions; examples employing nuclear magnetic resonance. *Nature, Lond.* **242**, 190.

Mansfield, P. 1971 Symmetrized pulse sequences in high resolution NMR in solids. *J. Phys.* C **4**, 1444.

Mansfield, P. & Grannell, P. K. 1973 NMR 'diffraction' in solids? *J. Phys.* C **6**, L422.

Mansfield, P & Grannell, P. K. 1975 'Diffraction' and microscopy in solids and liquids by NMR. *Phys. Rev.* B **12**, 3618.

Mansfield, P., Grannell, P. K., Garroway, A. N. & Stalker, D. C. 1973 Multi-pulse line narrowing experiments: NMR 'diffraction' in solids? *Proc. 1st Spec. Colloque Ampere* (ed. J. W. Hennel), p. 16. Krakow.

McDonald, P. J., Attard, J. J. & Taylor, D. G. 1987 A new approach to NMR imaging of solids. *J. magn. Reson.* **72**, 224.

McDonald, P. J. & Tokarczuk, P. F. 1989 An NMR multiple pulse sequence for the imaging of solids using sinusoidally driven magnetic field gradients. *J. Phys.* E **22**, 948.

Mehring, M. 1983 *Principles of high resolution NMR in solids*, 2nd edn. New York: Springer-Verlag.

Miller, J. B. & Garroway, A. N. 1986 Removal of static field inhomogeneities and chemical-shift effects in NMR imaging. *J. magn. Reson.* **67**, 575.

Miller, J. B. & Garroway, A. N. 1989*a* ^{1}H-refocussed gradient imaging of solids. *J. magn. Reson.* **82**, 529.

Miller, J. B. & Garroway, A. N. 1989*b* ^{13}C refocussed gradient imaging of solids. *J. magn. Reson.* **85**, 255.

Miller, J. B. & Garroway, A. N. 1989*c* Dipolar decoupled inversion pulses for NMR imaging of solids. *J. magn. Reson.* **85**, 432.

PHILOSOPHICAL TRANSACTIONS OF THE ROYAL SOCIETY A MATHEMATICAL, PHYSICAL & ENGINEERING SCIENCES

PHILOSOPHICAL TRANSACTIONS OF THE ROYAL SOCIETY A MATHEMATICAL, PHYSICAL & ENGINEERING SCIENCES

Downloaded from rsta.royalsocietypublishing.org

Miller, J. B., Cory, D. G. & Garroway, A. N. 1989 Pulsed field gradient NMR imaging of solids. *Chem. Phys. Lett.* **164**, 1.

Nieminen, A. O. K. & Koenig, J. L. 1989 NMR imaging of the interfaces of epoxy adhesive joints. *J. Adh. Sci.* **30**, 47.

Pines, A. & Waugh, J. S. 1972 Quantitative aspects of coherent averaging. Simple treatment of resonance offset processes in multiple pulse NMR. *J. magn. Reson.* **8**, 354.

Rhim, W.-K., Elleman, D. D. & Vaughan, R. W. 1973*a* Enhanced resolution in solid state NMR. *J. chem. Phys.* **58**, 1772.

Rhim, W.-K., Elleman, D. D. & Vaughan, R. W. 1973*b* Analysis of multiple pulse NMR in solids. *J. chem. Phys.* **59**, 3740.

Rommel, E., Hafner, S. & Kimmich, R. 1990 NMR imaging of solids by Jeener–Broekaert phase encoding. *J. magn. Reson.* **86**, 264.

Rothwell, W. P., Holecek, D. R. & Kershaw, J. A. 1984 NMR imaging: study of fluid adsorption by polymer composites. *J. Polym. Sci. Lett.* **22**, 241.

Samoilenko, A. A., Artemov, D. Yu. & Sibeldina, L. A. 1987 The application of NMR imaging to the study of the internal structures of solids. *Russ. J. Phys. Chem.* **61**, 1623.

Samoilenko, A. A., Artemov, D. Yu. & Sibeldina, L. A. 1988 Formation of sensitive layer in experiments on NMR subsurface imaging of solids. *JETP Lett.* **47**, 348–350.

Szeverenyi, N. M. & Maciel, G. 1984 NMR spin imaging of magnetically dilute nuclei in the solid state. *J. magn. Reson.* **60**, 460.

Turner, R. 1988 Minimum inductance coils. *J. Phys.* E **21**, 948.

Veeman, W. S. & Cory, D. G. 1989 ^{1}H NMR imaging of solids with magic angle spinning. *Adv. magn. Reson.* **14**, (2) (ed. W. Warren). Academic Press.

Wind, R. A. & Yannoni, C. S. 1979 Selective spin imaging in solids. *J. magn. Reson.* **36**, 269.

Discussion

P. Mansfield (*University of Nottingham, U.K.*). Dr Garroway emphasized the use of MREV-8 multipulse cycles together with modifications to achieve improved spatial resolution images. These sequences are partly permuted cycles, but fully permuted cycles are possible with potentially greater line narrowing efficiency. Does he see any potential for further improvement in spatial resolution using more complex line narrowing sequences? What would be the highest *practical* spatial resolution expected?

A. N. Garroway. Most of our experience in imaging has indeed been with the MREV-8 sequence, for circumstances in which we wish to preserve chemical shift information. We have not found major improvements in using partly permuted sequences or the Burum Rhim BR-24 sequence for imaging applications. However, when the chemical shift is not essential, then substantially improved resolution is achieved by removing *all* the chemical shift-like terms (susceptibility, magnetic inhomogeneity and some dipolar error terms). In addition to the methods I discussed in this paper, my colleague Dr D. G. Cory has found that longer, compensated versions of the eight-pulse sequence of Mansfield & Grannell (1975) provide major improvements in residual line width: for example, for ferrocene the proton dipolar line width is about 19 kHz; this is reduced to 45 Hz for the second averaged MREV-8 sequence and to 5.5 Hz for a 48-pulse version of the Mansfield–Grannell sequence. I should emphasize that there is no particular reason to take heroic measures to reduce the residual line width to its absolute minimum: in imaging, one can always turn up the strength of the gradient, at some penalty in the signal-to-noise ratio.

PHILOSOPHICAL TRANSACTIONS OF THE ROYAL SOCIETY A MATHEMATICAL, PHYSICAL & ENGINEERING SCIENCES
PHILOSOPHICAL TRANSACTIONS OF THE ROYAL SOCIETY A MATHEMATICAL, PHYSICAL & ENGINEERING SCIENCES

Downloaded from rsta.royalsocietypublishing.org

Although we are still far from resolution limits imposed by T_1 or $T_{1\rho}$, these residual line widths are now comparable with line widths accessible in conventional MRI. Therefore the resolution achievable in solids should be broadly comparable with that achievable in liquids, and hence be determined by signal-to-noise limitations. I would not wish to predict exactly the size of the smallest voxel achievable in solid state imaging: earlier estimates (Mansfield & Grannell 1975) have pointed out that despite the technical problems of line narrowing, one advantage to solid state imaging is that spatial information is not smeared out by molecular diffusion, much less by large-scale coherent motions.

D. J. GREENSLADE. Many industrial systems and materials contain free radicals; for example graphite fibre reinforced composites and even simple polymers. These might give difficulties in terms of relaxation times and even observability of some nuclei, but irradiation at other frequencies might lead to more or better information. Has Dr Garroway considered this?

A. N. GARROWAY. We have not worked in this area. The presence of the free radical can be, in principle, of great advantage. ESR imaging is one approach, though the level of free radicals in many polymeric systems is not high. Related to ESR imaging is some intriguing work by Professor J. Schaefer at Washington University (St Louis, Missouri) in which those nuclei proximate to free radicals near graphite fibres are excited by electron-nuclear double-resonance methods: it is the chemistry of the free radicals which provides the spatial localization, rather than any conventional imaging technique. Of course, with any of these methods, one must get the RF or microwave power into the sample, and that can be a problem for graphite reinforced composites if the sample geometry is not favourable. An intriguing possibility is raised: could broadband irradiation excite those nuclear spins not normally observed due to hyperfine broadening of nearby radicals and could the effects of this saturation be conveyed via spin diffusion to the observable nuclei, in a rough analogy with the saturation transfer approach in MRI?

K. J. PACKER (*BP Research, Sunbury-on-Thames, U.K.*). In the last slide Dr Garroway mentioned some 'easier' systems to which the methods he describes might be applied. In some of these the spins may well be in a motionally narrowed state with motional frequencies of the order of the inverse of his pulse separations. What strategies can one adopt to generating images in such circumstances?

A. N. GARROWAY. Professor Packer refers to the infelicitous circumstance in which the motional narrowing is sufficiently slow so that the static NMR line width is not greatly reduced, but fast enough to provide a very short rotating frame relaxation rate, which will ultimately limit the line-narrowing efficiency of the coherent averaging sequence. In polymers the distribution of motional correlation times and the anisotropic averaging will lead to a rather shallow 'depth' for this $T_{1\rho}$ minimum. We have not yet encountered samples where this circumstance is a serious problem: I suppose the most straightforward approach on confronting a deep minimum is to move to another temperature.

R. D. FARRANT (*Wellcome Foundation Ltd, Beckenham, U.K.*). What is the achievable spatial resolution with monopole magnet and surface coil combinations?

Downloaded from rsta.royalsocietypublishing.org

A. N. Garroway. Our experience is limited to a surface coil in a nominally homogeneous magnet. We have not attempted to push for higher spatial resolution. In solid state results with a 27 mm od circular surface coil we found a 200 μm resolution near the rf field. For liquid state imaging with a meander line rf coil (38×61 mm with a 1.5 mm wire spacing) resolution was about 100 μm. As the resolution of the meander line coil is determined by the wire spacing, substantially improved resolution should be possible for smaller wire spacing. Using a homogeneous rf field and a very inhomogeneous static field, created in the fringe field of a superconducting magnet, Samoilenko *et al.* (1978, 1988) report 100 μm resolution for solids. This later approach has recently been made commercial by Bruker Instruments.

J. H. Strange (*University of Kent, U.K.*). Most work in solids so far has concentrated on spin-density mapping. Does Dr Garroway envisage the development of relaxation-time mapping and will this fit into the multipulse line-narrowing methods? Are there potential difficulties with T_2 as opposed to T_1 or $T_{1\rho}$ as a characterizing parameter?

A. N. Garroway. Certainly relaxation time mapping is at the heart of the contrast mechanism in any nmr imaging, and one of the rationales for the present work is to unearth methods that will allow one to image from the most rigid to the most liquid-like material. The standard MREV-8 sequence already includes some relaxation time weighting, involving rotating frame spin-lattice and spin-spin effects: to some extent, one can emphasize one or the other by altering rf power or cycle time. It may be cleaner to perform the relaxation time weighting (T_1, $T_{1\rho}$, or T_2) before the line narrowing sequence. Having the facility to execute line narrowing also opens up some other possibilities to separate rigid from less rigid areas: one could select spins with certain relaxation times while suppressing the homogenizing effects of spin diffusion.

J. Frahm (*MPI für biophysikalische Clinic, Göttingen, F.R.G.*). Let us assume that all technical problems have been solved. What is it that Dr Garroway really wants to image? What is the information that can be extracted, in particular after having eliminated all the useful interactions by line narrowing?

A. N. Garroway. We certainly are *not* attempting to remove all useful interactions. Compared with our liquid-state colleagues who suffer irrevocable loss of useful information by motional averaging, we have a surfeit of information in solids and we are examining a host of techniques for switching off unwanted parts of the spin hamiltonian and, in return, achieving greater signal-to-noise and greater spatial resolution. The control over the relevant hamiltonian should not be underestimated: for example, though I indicated how to shut off the chemical shift during the line-narrowing sequence (and thereby remove uninteresting bulk susceptibility and static field broadening), that chemical shift information is still present and can be recalled at will, perhaps as chemical shift selection by a Dante sequence. Now to the more central question: what should be imaged? There are a number of intriguing possibilities: can one sufficiently discriminate relaxation times to map out the spatial variations in the glass transition temperature of a thermosetting polymer in a complex part? What are the size distributions and connectivities of defects in ceramics, composites or oil-bearing rock? How does a solvent move into an

PHILOSOPHICAL TRANSACTIONS OF THE ROYAL SOCIETY A MATHEMATICAL, PHYSICAL & ENGINEERING SCIENCES
PHILOSOPHICAL TRANSACTIONS OF THE ROYAL SOCIETY A MATHEMATICAL, PHYSICAL & ENGINEERING SCIENCES

Downloaded from rsta.royalsocietypublishing.org

inhomogeneous, anisotropic composite? Suitably modified MRI methods are already providing useful information for green ceramics and oil cores, two areas of materials sciences which do not immediately require line-narrowing methods. But it is certainly correct that the rationale for solid state methods, especially these line-narrowing methods, has not yet been justified by important practical demonstrations.

E. L. HAHN (*University of California at Berkeley, U.S.A.*). By use of the pulse sequence method at what point in the narrowing process, if at all, does the susceptibility effect of the surface come into play? Is it expected to average out in the same way the dipolar interaction is reduced? As pulse sequence narrowing reduces the solid to a pseudo-liquid, does Dr Garroway ever worry about the interference of accumulated echoes that result from the pulse sequence which precedes the narrowing?

A. N. GARROWAY. Some of the sequences I presented do indeed remove susceptibility broadening terms: the implicit assumptions are that any such susceptibility term be linear in the spin operator I_z over the timescale of the pulse cycle and that the magnitude of the RF pulse be larger than the strength of the susceptibility interaction. For organic materials with characteristic bulk susceptibilities of about 1 p.p.m., the susceptibility term is fairly small and well behaved: it does not have the additional complications of the homonuclear dipolar flip–flop term which gives the dipolar line shape its homogeneous character and, correspondingly, requires coherent averaging on the timescale of the flip–flop term. To a stroboscopic observer of the spin evolution, these coherent averaging methods have turned the solid into a pseudo-liquid: over short times, between the RF pulses, the dipolar couplings are essentially unmodified. The 'magic echo' may be closest in spirit to the effect you ask about. There an RF pulse sequence of duration τ ($\tau > T_2$) causes the dipolar system to evolve at $(-\frac{1}{2})$ of its laboratory frame rate for the homonuclear dipolar coupling. Following the turn-off of the sequence, no magnetization is seen until an additional time $\frac{1}{2}\tau$, when an echo magically appears. Under dipolar coupling the magnetization, a single-quantum coherence, evolves into multiple-quantum coherences, with corresponding 'loss' of magnetization. This multiple-quantum evolution is reversible to a high degree and, during the second interval in the magic echo experiment, the higher-order coherences evolve backwards in time to re-create the magnetization as an echo. I should also mention that the RF power levels in these line-narrowing experiments are rather high, and many workers have inadvertently succeeded in turning their solids into real liquids and, sometimes, to gases.

PHILOSOPHICAL TRANSACTIONS OF THE ROYAL SOCIETY A MATHEMATICAL, PHYSICAL & ENGINEERING SCIENCES
PHILOSOPHICAL TRANSACTIONS OF THE ROYAL SOCIETY A MATHEMATICAL, PHYSICAL & ENGINEERING SCIENCES

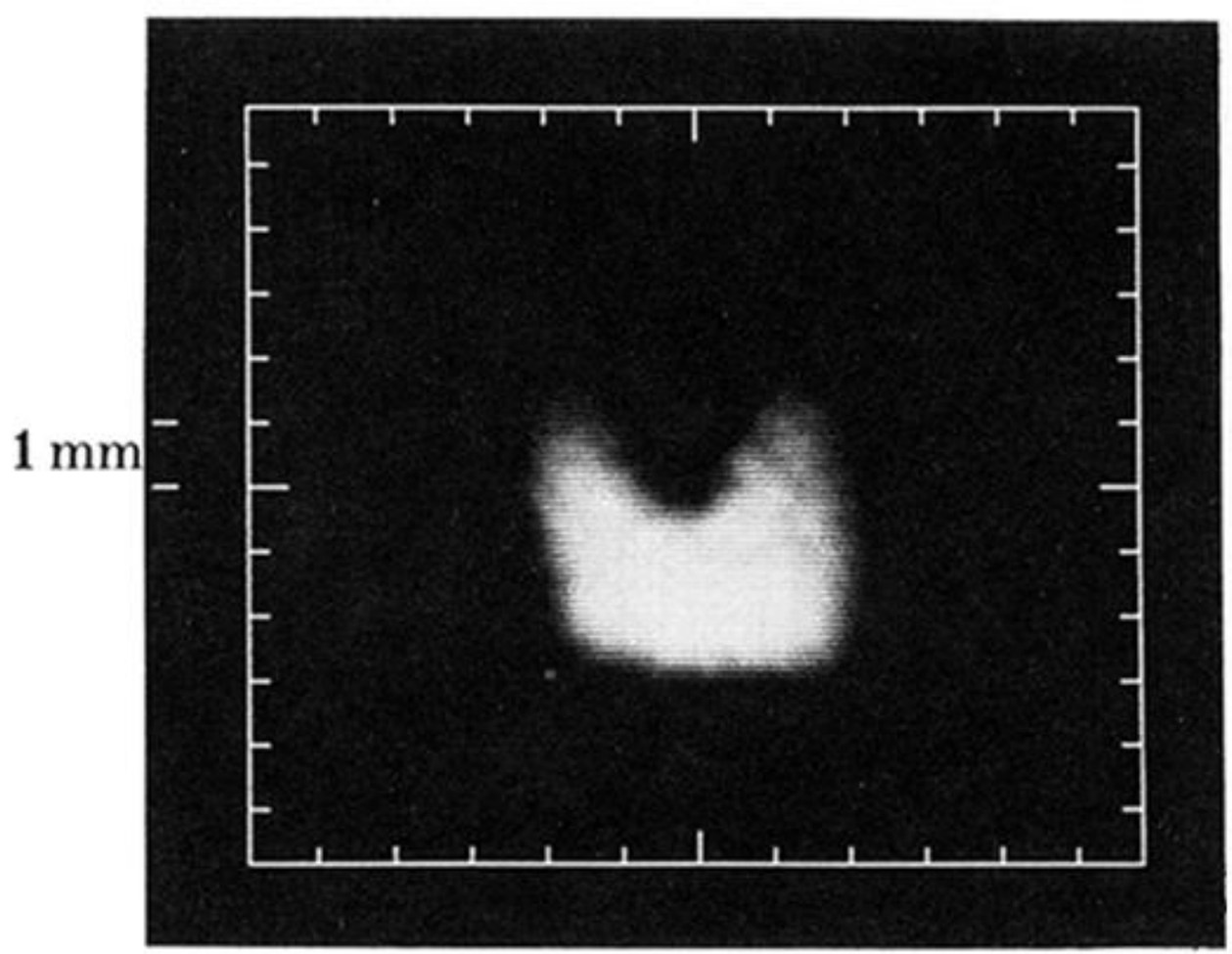

gure 1. Two-dimensional ^1H image of a polyacrylic specimen of dimensions $4.5 \times 5.5 \times 16$ mm. A otch has been cut out parallel to the long direction. The image was obtained by back projection om 18 projections and no slice selection was employed. The refocused gradient methods for omonuclear (Miller & Garroway 1989*a*) spin systems remove chemical shift-like interactions, as ell as the respective dipolar couplings. For the homonuclear decoupling sequence used here, the sidual line width depends on the resonance offset and therefore the spatial resolution deteriorates ross the image: the present paper is concerned with remedies to this effect.

PHILOSOPHICAL TRANSACTIONS OF THE ROYAL SOCIETY A MATHEMATICAL, PHYSICAL & ENGINEERING SCIENCES

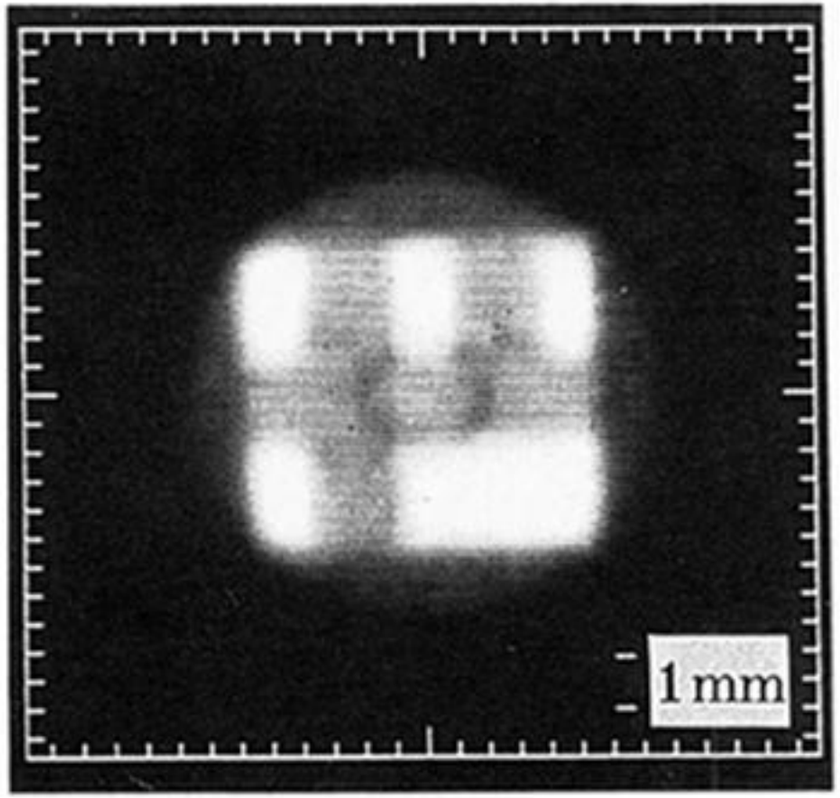

gure 5. Refocused gradient imaging with pulsed gardients was used to obtain a proton image of
Ultem (polyether imide) phantom, comprising a circular base 9 mm in diameter by 1.9 mm
ick, a rectangular layer $6.2 \times 6.5 \times 2.0$ mm thick, and a second layer of smaller rectangles parallel
the rectangle in the first layer. The smaller rectangles are 2.2 mm thick and are separated from
ch other by 1.6 mm. No slice selection was used and so the small rectangles appear against the
ckground of the larger rectangle and the cylindrical section. A 16-pulse sequence (Cho *et al.* 1985)
s been used for refocused gradient imaging of solids and is based on a sequence proposed by
ansfield & Grannell (1975). Resolution is 160 μm.

PHILOSOPHICAL TRANSACTIONS OF THE ROYAL SOCIETY A MATHEMATICAL, PHYSICAL & ENGINEERING SCIENCES

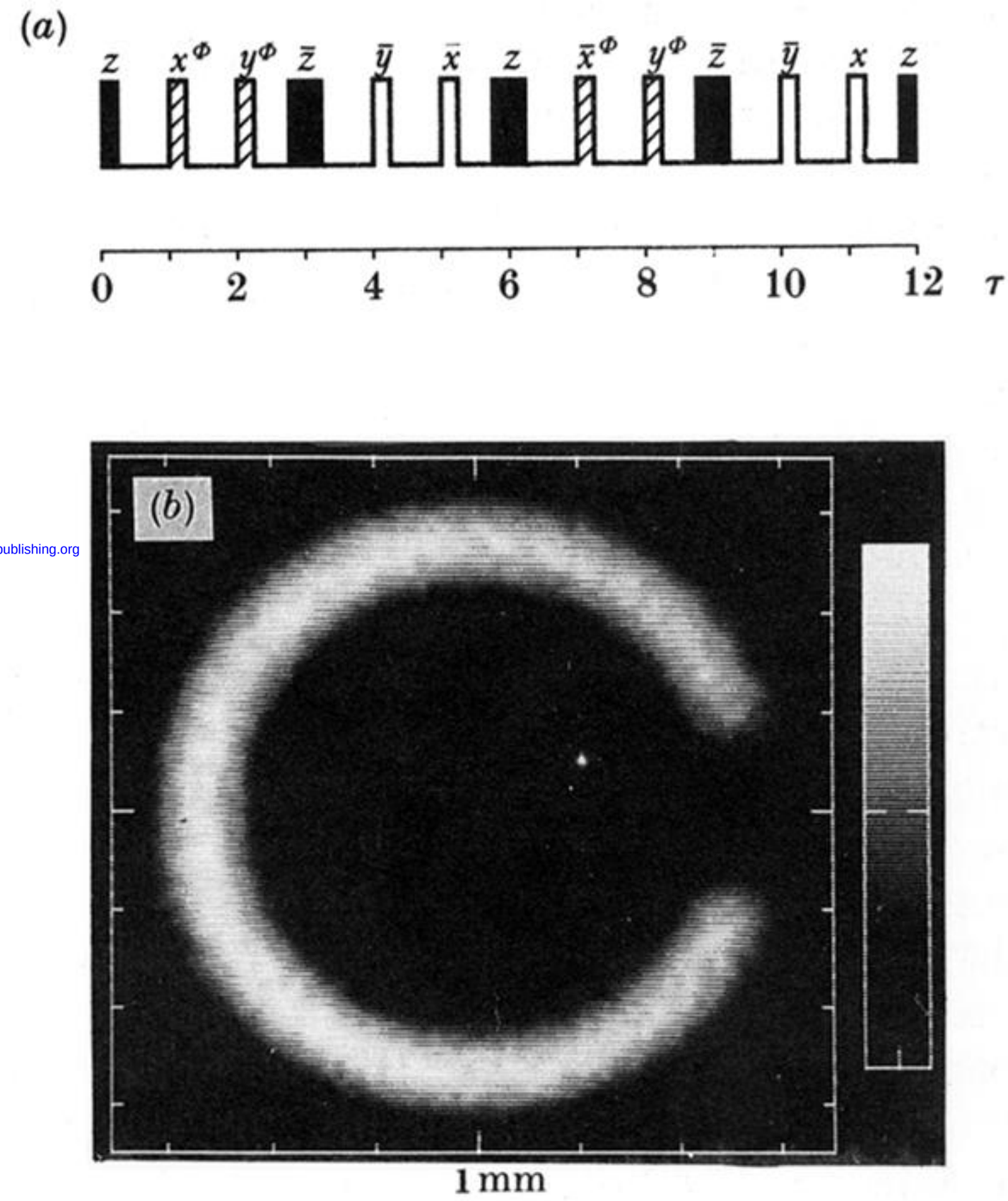

Downloaded from rsta.royalsocietypublishing.org

igure 7. Proton solid state imaging (Cory *et al.* 1990) by second averaging. The MREV-8 RF pulse quence, top, is modified for second averaging and imaging. To induce second averaging of the emical shift, susceptibility and magnet inhomogeneity terms which appear as $(I_z - I_x)$ about an thogonal axis, $(I_z + I_x)$, a phase toggle Φ is applied to pairs of RF pulses as indicated: x^{Φ} denotes $\frac{1}{2}\pi$ RF pulse which has been advanced by Φ from the x axis. The position and polarity of the adient pulses, z and $\bar{z}$, are also arranged to produce an effective field about $(I_z + I_x)$ and so the emical shift-like terms are second averaged by the sum of the gradient and the phase shift terms. lso shown is the ^{1}H image of a 6.35 mm OD poly(methyl methacrylate) cylinder from which a 59 mm slot has been machined. No slice selection was used. The image was reconstructed from back projections.

PHILOSOPHICAL TRANSACTIONS OF THE ROYAL SOCIETY A MATHEMATICAL, PHYSICAL & ENGINEERING SCIENCES